

Supplementary Information

Optical Control of Mitochondrial Reductive Reactions in Living Cells using an Electron Donor-Acceptor Linked Molecule

Yuta Takano,^{*a,b} Reina Munechika,^c Vasudevan Pillai Biju,^b Hideyoshi Harashima,^c Hiroshi Imahori,^{*a,d} and Yuma Yamada^{*c}

^a*Research Institute for Electronic Science, Hokkaido University, Kita-20 Nishi-10, Kita-ku, Sapporo 001-0020, Japan.*

^b*Institute for Integrated Cell-Material Sciences (WPI-iCeMS), Kyoto University, Sakyo-ku, Kyoto 606-8501, Japan.*

^c*Laboratory for Molecular Design of Pharmaceuticals, Faculty of Pharmaceutical Sciences, Hokkaido University, Kita-12 Nishi-6, Kita-ku, Sapporo 060-0812, Japan.*

^d*Department of Molecular Engineering, Graduate School of Engineering, Kyoto University, Nishikyo-ku, Kyoto 615-8510, Japan.*

*Correspondence to: (Y.T.) ytakano@icems.kyoto-u.ac.jp, (H.I.) imahori@scl.kyoto-u.ac.jp, (Y.Y.) u-ma@pharm.hokudai.ac.jp,

Materials and methods

Materials:

C₆₀ (99.98%) was obtained from MTR Ltd. (OH, USA), and was used as-received. COATSOME EL-11-A (NOF co., Tokyo, Japan) (Lipid composition: POPC:Cholesterol:POPG = 30:40:30 mol%. unilamellar vesicle with high monodispersity) was obtained from NOF Co. (Japan). All other solvents and chemicals were of reagent-grade quality, were purchased commercially, and were used without further purification unless otherwise noted. Dulbecco's phosphate buffered saline (PBS) and Hank's Balanced Salt Solution (HBSS) were obtained from Thermo Fisher Scientific Inc. (MA, USA). Cell culture dishes and glass bottom dishes were purchased from Corning Inc. (MA, USA).

General Procedures:

¹H NMR spectra were measured by a JEOL JNM-EX400 NMR spectrometer or a Bruker AVANCE 500 spectrometer, where TMS was used as an internal reference ($\delta = 0.00$ ppm). Matrix-assisted laser desorption/ionization (MALDI) time-of-flight mass spectra were obtained using a SHIMADZU Biotech AXIMA-CFR with 1,8-dihydroxy-9(10H)-anthracenone (dithranol) as a matrix for the negative mode and positive mode, respectively. IR spectra were recorded on a JASCO FT/IR-470 Plus spectrometer. UV-vis-near infrared (NIR) spectra were measured with a Perkin-Elmer Lambda 900 spectrometer. Steady-state fluorescence spectra were obtained by a HORIBA SPEX Fluoromax-3 spectrofluorometer or a HORIBA Jobin Yvon FluoroMax-4 spectrofluorometer. Electrochemical measurements were performed using a BAS ALS 630a electrochemical analyzer. A glassy carbon (3 mm diameter) working electrode, Ag/AgCl (sat. KCl) reference electrode, and Pt wire counter electrode were employed. Statistical analysis was performed using Igor Pro v6.3 using a one-way ANOVA with a Dunnett's post hoc test for significance.

Synthesis:

Compounds **1-Me**,¹ **ZnP-CHO**,¹ *N*-octylglycine,² **ref-Fc-ZnP-C₆₀-ref**,³ and **ref-ZnP**⁴ (Figs. S1 and S2) were synthesized according to the literature reports and were characterized based on spectral data.

2-Oct.

To a solution of C₆₀ (2.0 mmol) in toluene (20 mL), *N*-octylglycine (5.0 mmol), and **ZnP-CHO** (1.0 mmol) were added at room temperature. Under an argon atmosphere, the reaction mixture was refluxed for 10 h in the dark. The solution containing the crude product was allowed to cool to room temperature and evaporated to dryness under reduced pressure, and the residue was purified by column chromatography on silica gel to yield the desired product **3** as a purple solid (10.5 mg, 3.93 μ mol, 70 %). ¹H NMR (400 MHz, CDCl₃): δ 8.82 (d, *J* = 4 Hz, 2H), 8.81 (d, *J* = 4 Hz, 2H), 8.68 (d, *J* = 12 Hz, 4H), 8.30-8.05 (m, 8H), 8.02 (s, 1H), 7.89-7.78 (m, 4H), 7.69 (s, 1H), 7.62 (t, *J* = 8 Hz, 2H), 7.52 (d, *J* = 8 Hz, 1H), 7.17 (d, *J* = 8 Hz, 2H), 7.10 (d, *J* = 8 Hz, 2H), 7.01 (d, *J* = 8 Hz, 2H), 6.92 (d, *J* = 12 Hz, 4H), 4.97 (d, *J* = 2 Hz, 1H), 4.84 (s, 1H), 4.77 (m, 2H), 4.25 (m, 2H), 4.24 (d, *J* = 2 Hz, 1H), 4.11 (t, *J* = 6 Hz, 2H), 4.03 (s, 5H), 3.75 (t, *J* = 6 Hz, 8H), 3.41 (t, *J* = 6 Hz, 2H), 2.81 (s, 9H), 2.00-1.85 (CH₂, m, 4H), 1.60-1.50 (CH₂, m, 4H), 1.48-1.43 (CH₂, m, 12H), 1.30-1.14 (m, 8H), 1.00-0.67 (m, 32H), 0.65-0.50 (m, 15H), 0.50-

0.40 (m, 9H); FTIR (neat): ν 2919, 2849, 1655, 1680, 1593, 1518, 1455, 1246, 1097, 1070, 998, 819, 796, 754, 717 cm^{-1} ; HR mass (MALDI-TOF) calcd. for $\text{C}_{184}\text{H}_{157}\text{BrFeN}_7\text{O}_7\text{Zn}$ ($[\text{M}+\text{H}]^+$) 2774.997, found 2774.994 m/z .

1-Oct.

A solution of 33 wt.% NMe_3 in ethanol (0.03 mL) was added to a solution of **2-Oct** (10.0 mg, 3.74 μmol) in CHCl_3 (1.0 mL) with stirring at room temperature and the reaction mixture was stirred for 3 days. During the reaction, CHCl_3 (1 mL) and a NMe_3 solution (0.03 mL) were added every 24 h. The solution was then concentrated under reduced pressure and the product was precipitated by adding cyclohexane. The solid residue was washed with cyclohexane, cyclohexane / $\text{CH}_2\text{Cl}_2 = 1/1$ (v/v), then H_2O , followed by drying under a vacuum. The product **1-Oct** was obtained as a purple solid (8.1 mg, 3.3 μmol , 89% yield). ^1H NMR (500 MHz, $\text{DMSO}-d_6$, 60°C): δ 10.52 (NHCO, brs, 1H), 10.44 (NHCO, brs, 1H), 8.76–8.58 (m, 9H), 8.42–8.15 (m, 10H), 8.05–7.96 (m, 2H), 7.92–7.85 (m, 2H), 7.78 (brs, 2H), 7.64–7.58 (m, 2H), 7.48–7.42 (m, 2H), 7.12–7.03 (m, 4H), 5.13 (brs, 1H), 5.10 (brd, 1H), 4.87 (Fc, brs, 2H), 4.36 (Fc, brs, 2H), 4.15 (brt, 4H), 4.08 (Fc, brs, 5H), 3.81 (ArOCH₂, m, 8H), 3.36–3.29 (OCH₂, m, 2H), 3.07 (N⁺(CH₃)₃, s, 9H), 2.81 (NCH₃, s, 3H), 2.63 (OCH₂CH₂, m, 1H), 2.35 (OCH₂CH₂, m, 1H), 2.00–1.92 (CH₂, m, 2H), 1.84–1.72 (CH₂, m, 4H), 1.68–1.59 (CH₂, m, 2H), 1.50–1.45 (m, 2H), 1.30–1.20 (m, 4H), 0.97–0.79 (m, 26H), 0.74–0.65 (m, 6H), 0.61–0.47 (m, 32H), 0.45–0.37 (m, 6H); FTIR (film): ν 3293, 2940, 2916, 2846, 1670, 1595, 1518, 1455, 1331, 1245, 1109, 1040, 994, 943, 793, 718 cm^{-1} ; HR mass (MALDI-TOF) calcd. for $\text{C}_{187}\text{H}_{165}\text{FeN}_8\text{O}_7\text{Zn}$ ($[\text{M}-\text{Br}]^+$): 2754.144, found 2754.145 m/z .

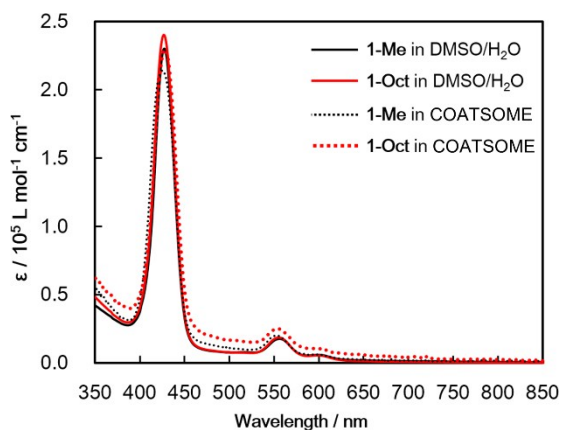
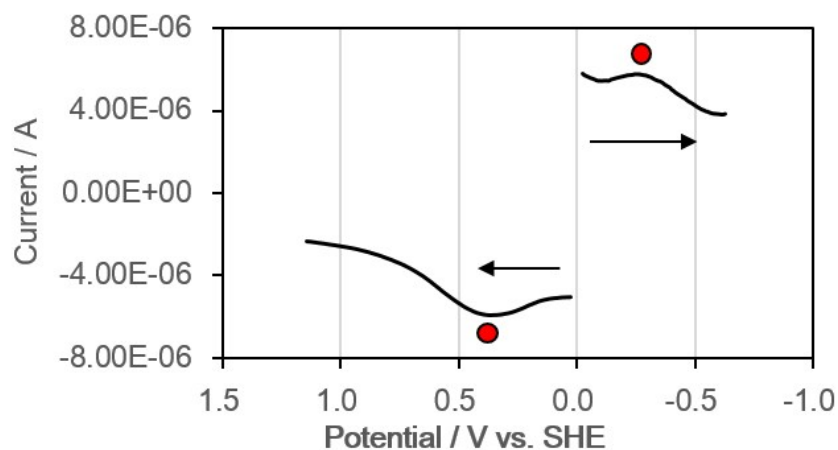


Fig. S3 Steady-state absorption spectra of **1-Me** and **1-Oct** in DMSO/H₂O (1/99, v/v) and in the COATSOME in H₂O.

(a)



(b)

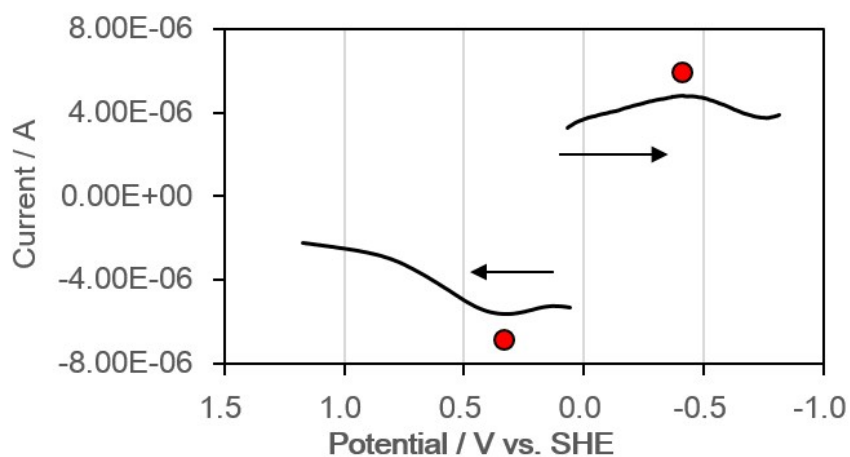
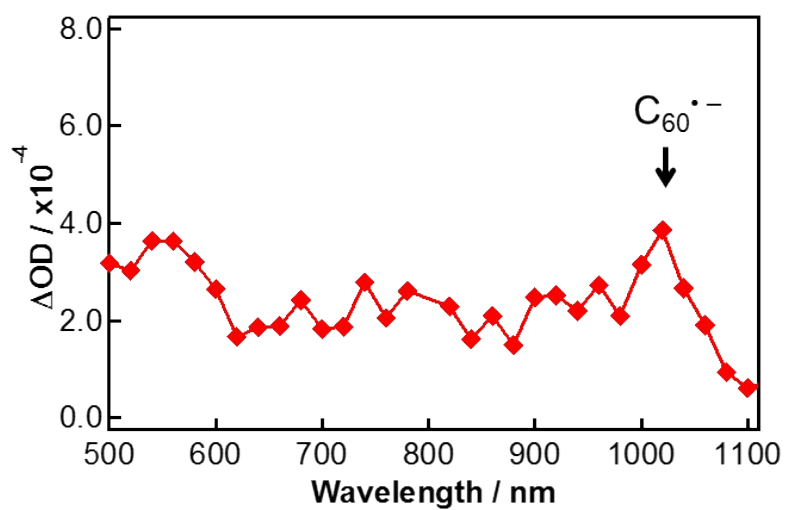


Fig. S4 Differential pulse voltammetry (DPV) of (a) **1-Me** and (b) **1-Oct**. Arrow marks indicate the direction of scans. Conditions: working electrode, glassy carbon; counter electrode, platinum wire; reference electrode, Ag/AgNO₃; supporting electrolyte: 0.020 M KCl in argon saturated H₂O; DPV: pulse amplitude, 50 mV; scan rate, 20 mV s⁻¹.

(a)



(b)

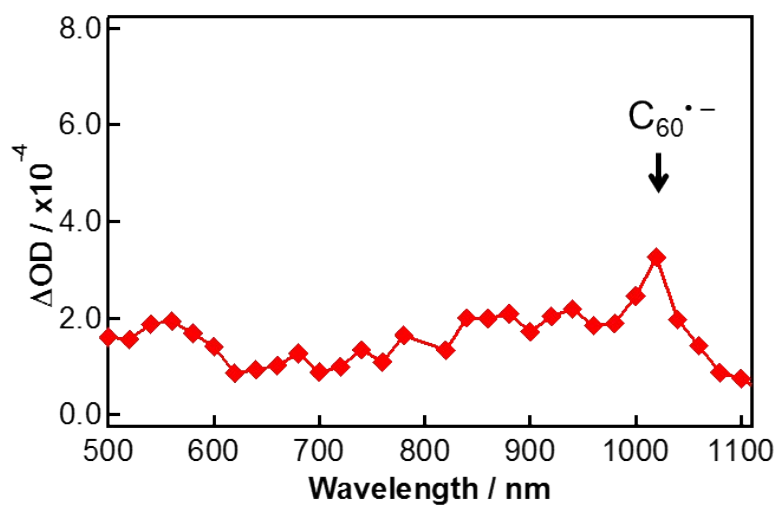


Fig. S5 Nanosecond time-resolved transient absorption (TA) spectra of (a) **1-Me** and (b) **1-Oct** in deaerated DMSO/H₂O (1/99, v/v) taken at 0.9 μ s after laser excitation by a 5.0 mJ pulse⁻¹ at 450 nm where the absorbances were adjusted to be identical (0.30).

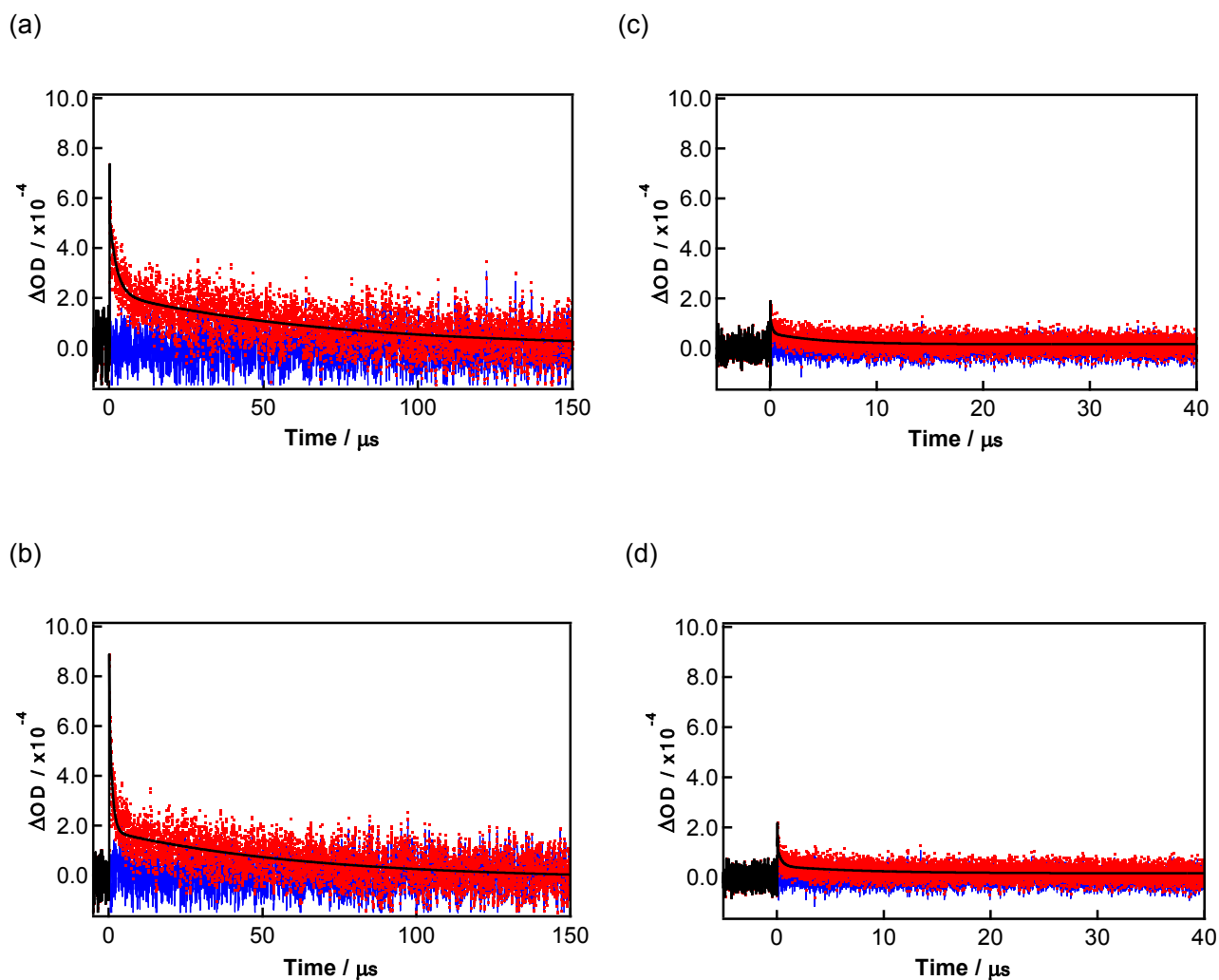


Fig. S6 Decay time profiles of (a, c) **1-Me** and (b, d) **1-Oct** at 1000 nm arising from $C_{60}^{\cdot-}$, which were obtained by nanosecond time-resolved TA measurements (a, b) in deaerated DMSO/H₂O (1/99, v/v) and (b, d) in aerated DMSO/H₂O (1/99, v/v), after nanosecond laser excitation. The profiles were obtained by excitation at 450 nm where the absorbances were adjusted to be identical (0.30). Red plots are the observed signals, black line represents the values obtained by bi-exponential fitting, and blue line is the residual after the fitting.

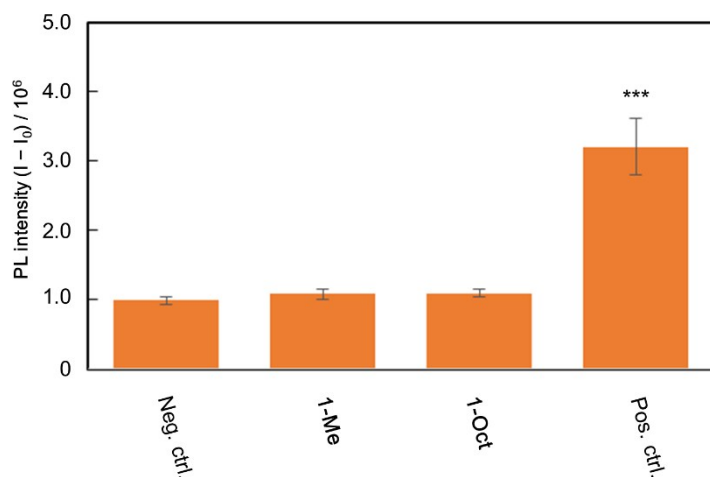
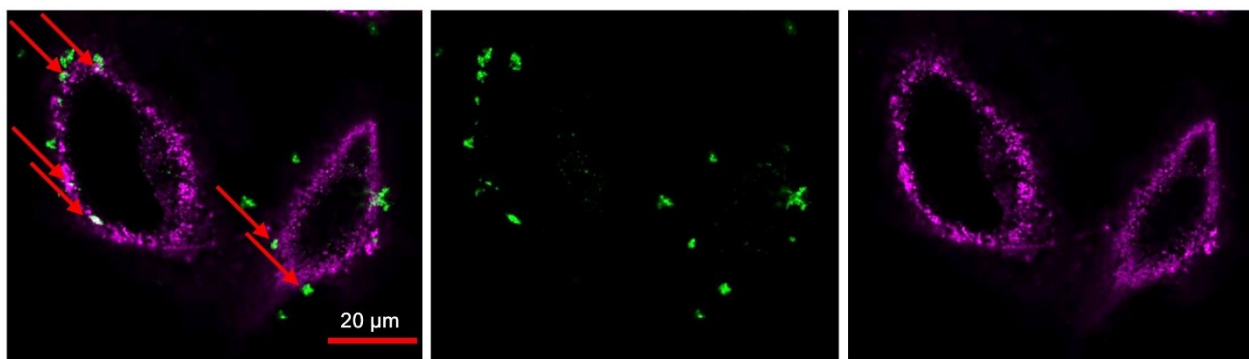
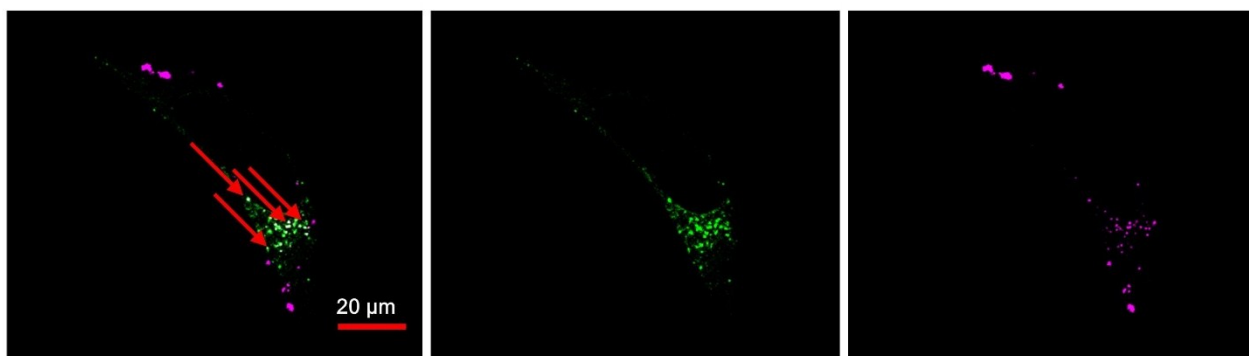


Fig. S7 Detection of singlet oxygen (¹O₂) by Singlet Oxygen Sensor Green (SOSG) in DMSO/H₂O (1/99, v/v). Conditions: Xe lamp wavelength, 430-440 nm, 400 mJ cm⁻². Error bars indicate S.D. (*n* = 3). Statistically significant differences between the negative control and each compound are indicated with asterisks (**P*<0.05, ****P*<0.001). **ref-ZnP** (Figure S1) was used for a positive control condition.

(a) 1-Oct + WGA-AlexaFluor488 : membrane lipids



(b) 1-Oct + LysoTracker Green DND-26 : lysosome



(c) neg/MP + MitoTracker® Green FM: mitochondria

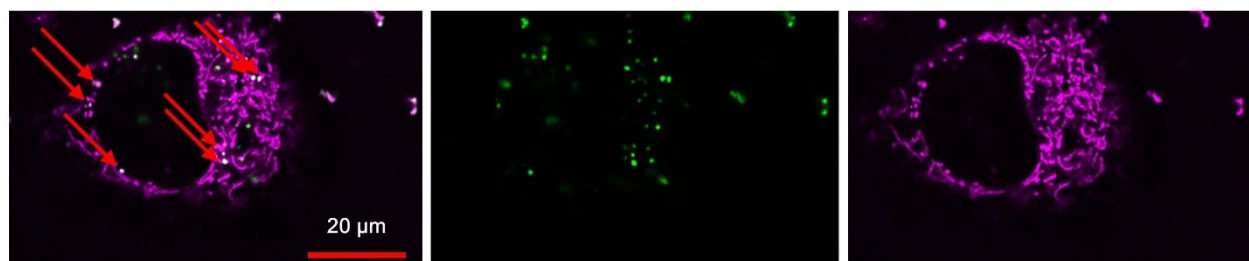


Fig. S8 Confocal microscopy images of HeLa cells (a) that were stained by wheat germ agglutinin (WGA)-Alexa Fluor488 conjugate with **1-Oct**, in the absence of MITO-Porter, (b) LysoTracker Green DND-26 with **1-Oct**, and (c) MitoTracker Green FM with **neg/MP**, which contains DiD. Merged image (left), compounds (green, center), and fluorescent reagents (magenta, right). Red arrows indicate strong overlapping points (white) of the compound and the fluorescent reagent.

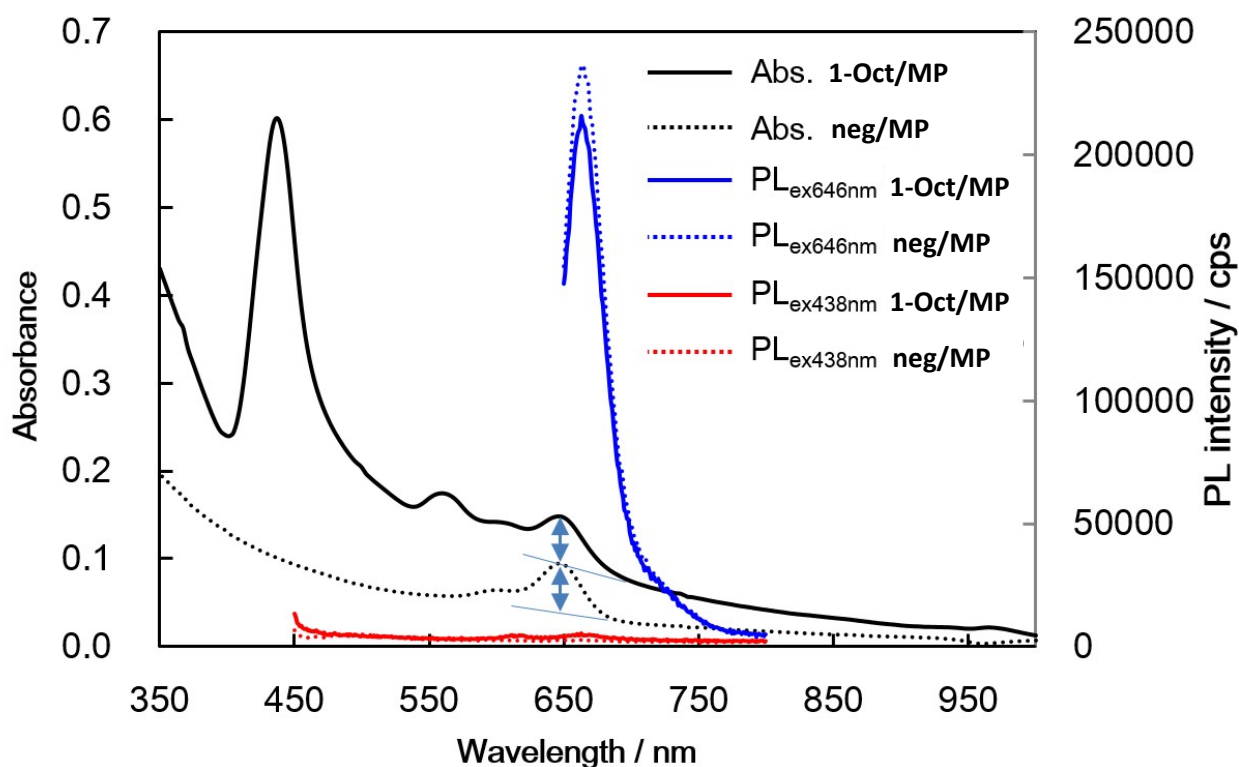


Fig. S9 UV-visible absorption spectra and fluorescent spectra of **1-Oct/MP** and **neg/MP** in H₂O. The fluorescence spectra were obtained by the excitation of the sample showing the present absorption spectra where the absorbances at 646 nm from DiD, which are indicated by arrow marks, were adjusted to be identical. These spectra ensure that fluorescence resonance energy transfer (FRET) from **1-Oct** to DiD does not occur in the MITO-Porter because the excitation at 438 nm did not enhance the fluorescence of DiD, which has a fluorescence peak at 660 nm.

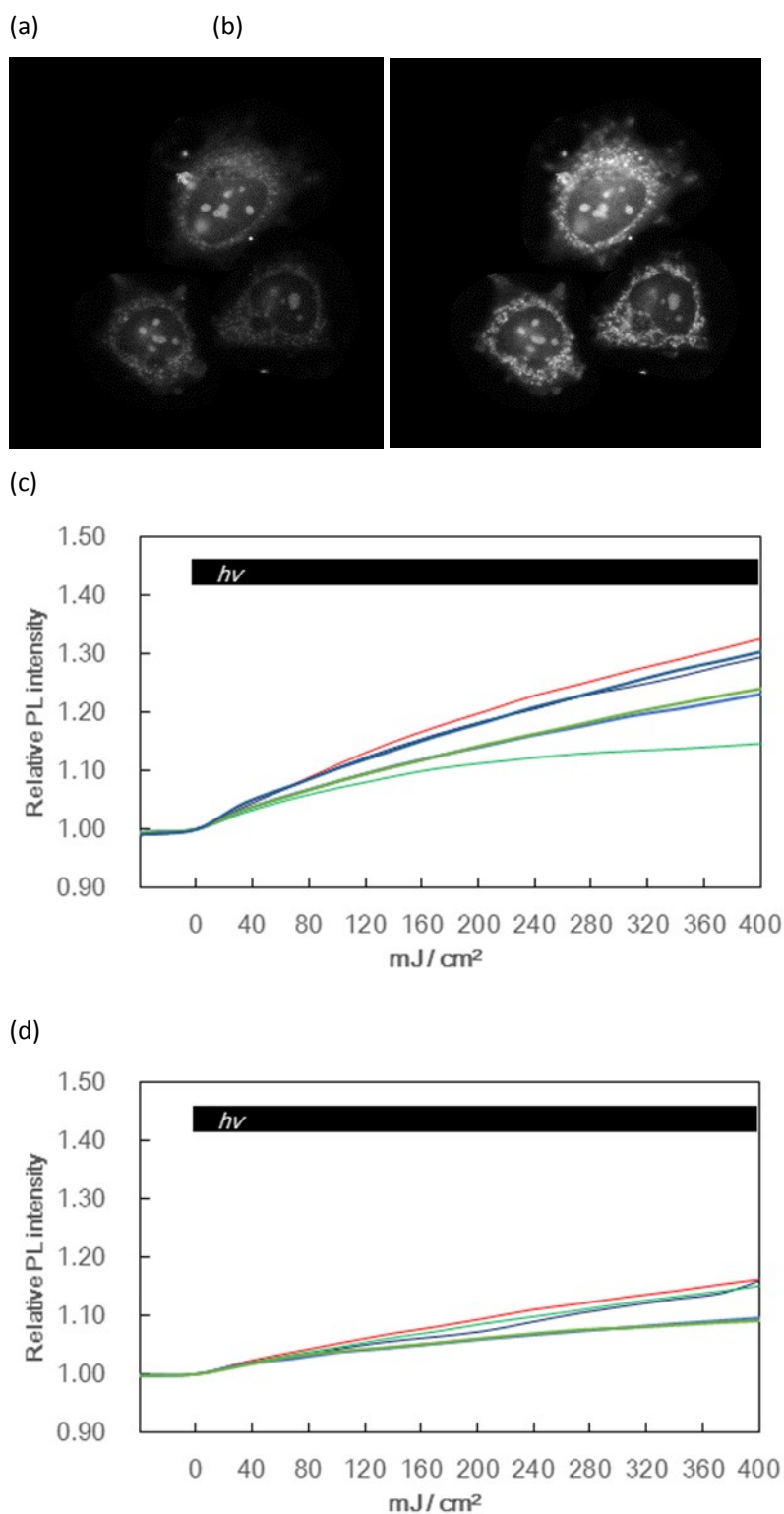


Fig. S10 Representative microscopic images of the ability to induce apoptosis of HeLa cells determined by the photoluminescence (PL) intensity change of MitoSOX (Figure 5c), (a) before and (b) after illumination (430-440 nm, 400 mJ cm⁻²). (c) Traces of the change upon the illumination with the treatment of **1-Oct/MP** (10 μM based on the lipids of **MP**). (d) Traces of the change upon the illumination with the treatment of **neg/MP** (10 μM based on the lipids of **MP**).

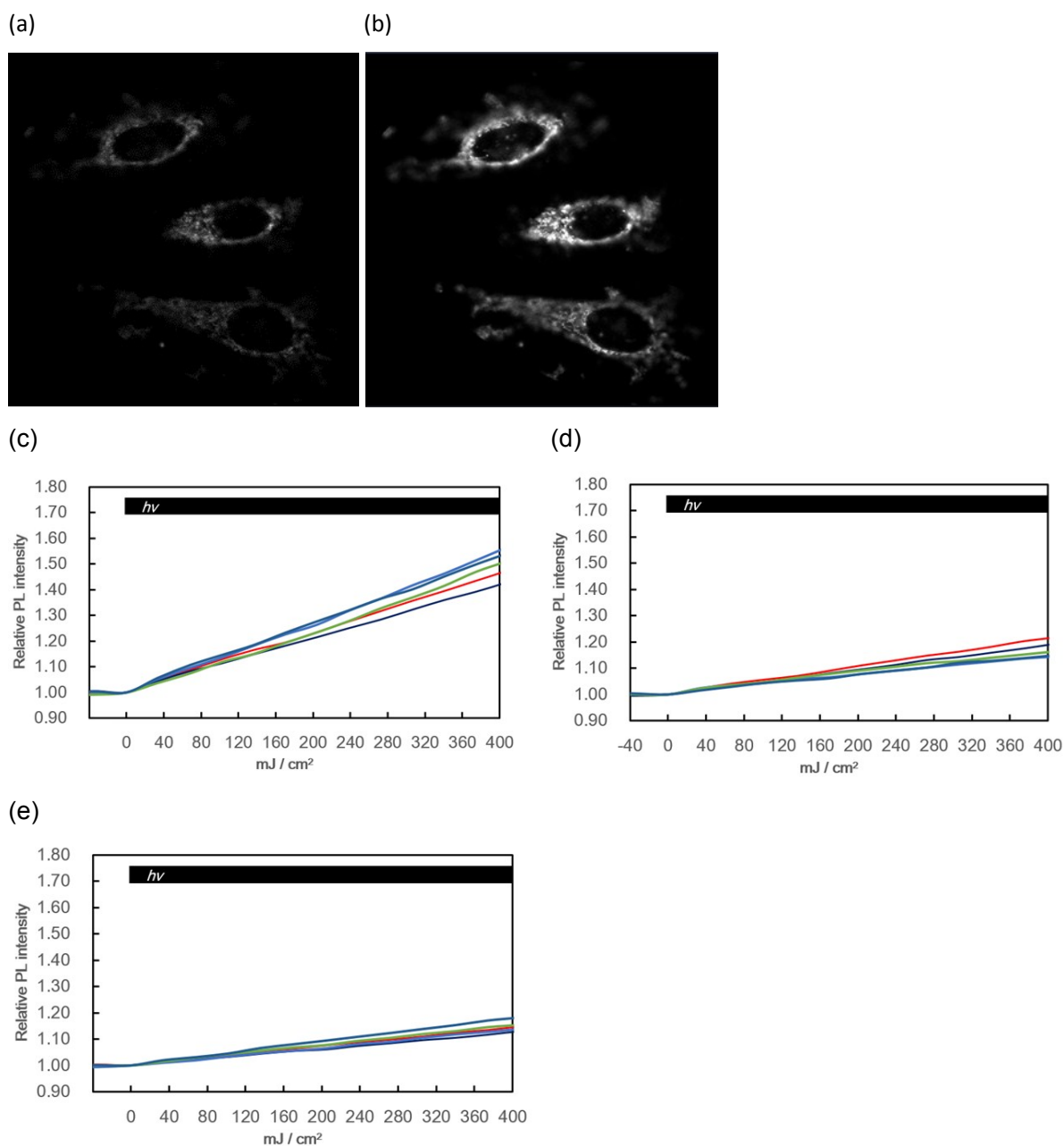


Fig. S11 Representative confocal laser microscopic images of the ability to generate reactive oxygen species (ROS), as determined by the photoluminescence (PL) intensity change of MitoTracker Orange CM-H2TMRos on HeLa cells in the mitochondria (Figure 6), (a) before and (b) after illumination (430-440 nm, 400 mJ cm⁻²). (c) Traces of the change upon illumination with the treatment of **1-Oct/MP** (10 μM based on the lipids of **MP**). (d) Traces of the change upon illumination with the treatment of **neg/MP** (10 μM based on the lipids of **MP**). (e) Traces of the change upon illumination with the treatment of **1-Oct/MP** (10 μM based on the lipids of **MP**) and MitoTEMPO.

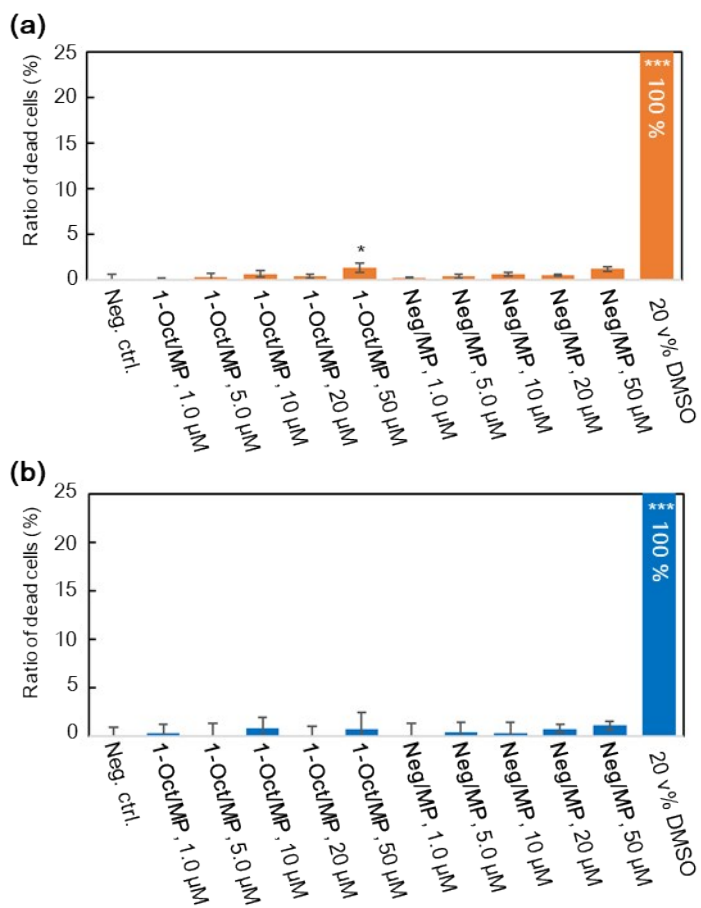
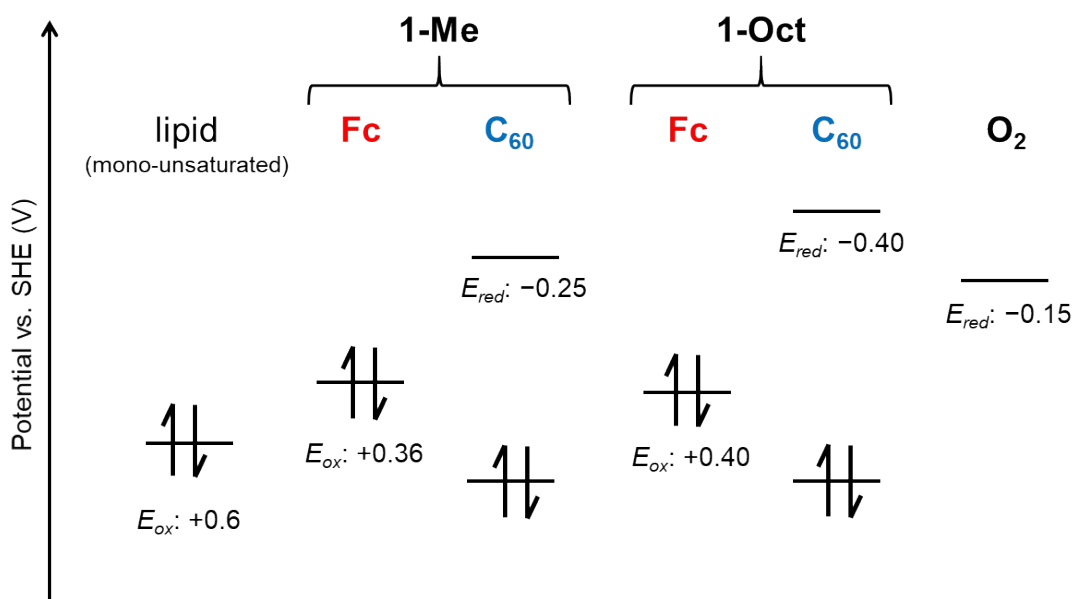


Fig. S12 Induction ability of late-apoptosis/necrosis of HeLa cells (a) with and (b) without illumination. *h* ν : 430-440 nm, 400 mJ cm⁻². Indicated concentrations are based on the lipids contained by the MITO-Porter. Error bars indicate S.D. (n = 4). Statistically significant differences between the negative control and each condition are illustrated with asterisks (*P < 0.05, ***P < 0.001). The positive control condition is the incubation of HeLa cells in culture medium containing 20 v% of DMSO for 2 h at 37°C prior to the assays.

Scheme S1. Energy diagram showing energy levels that were obtained from the electrochemical measurements shown in Figure S4 and Table S1. The oxidation potentials of cardiolipin (CL) were obtained from Ref. 5.



Scheme S2. Plausible path for the Intermolecular electron transfer reaction from **1-Oct** in its photoinduced charge separated state to ³O₂, based on the energy diagram shown in Scheme S1.

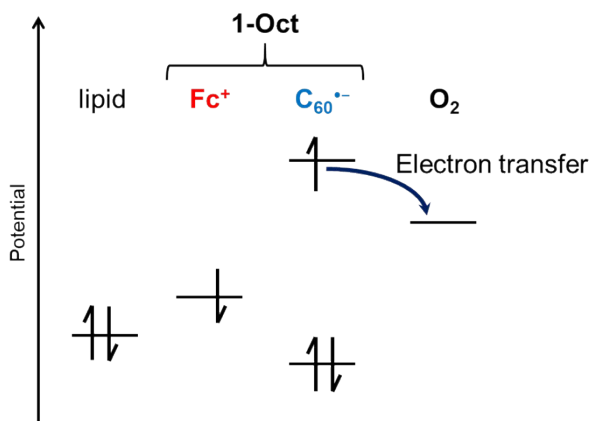


Table S1. Redox potentials.^{a,b}

compound	$E_{\text{ox}}^{(1)} / \text{V}$	$E_{\text{red}}^{(1)} / \text{V}$
1-Me	0.36	-0.25
1-Oct	0.40	-0.40
O ₂		-0.15

^a Values are in volts relative to a SHE and were obtained from DPV. ^b Conditions: working electrode, glassy carbon; counter electrode, platinum wires; reference electrode, Ag/AgCl; supporting electrolyte and solvent, 0.020 M KCl in H₂O; pulse amplitude, 50 mV; scan rate, 20 mV s⁻¹.

References:

1. Y. Takano, T. Numata, K. Fujishima, K. Miyake, K. Nakao, W. D. Grove, R. Inoue, M. Kengaku, S. Sakaki, Y. Mori, T. Murakami and H. Imahori, *Chem. Sci.*, 2016, **7**, 3331-3337.
2. Y. Takano, M. A. Herranz, N. Martin, S. G. Radhakrishnan, D. M. Guldi, T. Tsuchiya, S. Nagase and T. Akasaka, *J. Am. Chem. Soc.*, 2010, **132**, 8048-8055.
3. H. Imahori, K. Tamaki, D. M. Guldi, C. P. Luo, M. Fujitsuka, O. Ito, Y. Sakata and S. Fukuzumi, *J. Am. Chem. Soc.*, 2001, **123**, 2607-2617.
4. T. Numata, T. Murakami, F. Kawashima, N. Morone, J. E. Heuser, Y. Takano, K. Ohkubo, S. Fukuzumi, Y. Mori and H. Imahori, *J. Am. Chem. Soc.*, 2012, **134**, 6092-6095.
5. Y. Y. Tyurina, V. Kini, V. A. Tyurin, I. I. Vlasova, J. F. Jiang, A. A. Kapralov, N. A. Belikova, J. C. Yalowich, I. V. Kurnikov and V. E. Kagan, *Mol. Pharmacol.*, 2006, **70**, 706-717.